Interfacial and mechanical characterisation of biodegradable polymer-flax fibre composites

Delphin Pantaloni, Anton Loïc Rudolph, Darshil U. Shah, Christophe Baley, Alain Bourmaud

Interfacial and mechanical characterisation of biodegradable polymer-flax fibre composites

Delphin Pantaloni[1*], Anton Loïc Rudolph[2], Darshil U. Shah[3], Christophe Baley[1] and Alain Bourmaud[1]

[1] Université de Bretagne-Sud, IRDL, CNRS UMR 6027, BP 92116, 56321 Lorient Cedex, France

[2] City university of Applied Sciences, Dept. of Biomimetics, Neustadtswall 30, 28199 Bremen, Germany

[3] Centre for Natural Material Innovation, Department of Architecture, University of Cambridge, Cambridge CB2 1PX, United Kingdom

* Corresponding author: delphin.pantaloni@univ-ubs.fr. Tel.: +33-2-97-87-45-18

Abstract

Replacing glass fibres with flax fibres is a first step in reducing the ecological impact of thermoset composite materials, and employing a biodegradable thermoplastic matrix opens up recycling and composting as end-of-life routes. Here, a range of flax fibre reinforced biodegradable thermoplastics were investigated: poly-(hydroxy alkanoate) (PHA), poly-(butylene-succinate) (PBS) and poly-(lactide) (PLA). Poly-(propylene) (PP) and maleic-anhydride grafted poly-(propylene) (MAPP) were studied as industry benchmarks. This study systematically examines the interface between flax fibres and these matrices at multiple scales, and explores the correlations between the measured interfacial properties and macro-scale composite properties. Micro-droplet tests reveal that the adhesion of flax with biodegradable polymers is at least similar to flax-MAPP, and better than flax-PP. In-plane $[\pm 45]_s$ shear tests and tensile tests on unidirectional

composites reaffirm the observations at the micro-scale, that biodegradable polymer/flax composites present mechanical properties comparable to or better than MAPP/flax composites. Furthermore, comparison between interfacial and composite tensile properties reveals that fibre-matrix adhesion has a substantial role in biocomposite performance.

Keywords

A.Biocomposites; B.Interfaces; B.Mechanical properties; C. Compression Moulding

1. Introduction:

Due to their light weight and high mechanical properties, composites are nowadays used in many industrial sectors such as transport and construction. However, they often have a high environmental impact due to the choice of the polymer, as well as the reinforcement, glass and carbon fibres being the most commonly used. Replacing these synthetic fibres by plant fibres decreases the environmental impact of the composite [1]. Among them, flax fibres are widely chosen as their specific mechanical properties make them competitive against glass fibres [2] and opening the way to structural or semi-structural plant fibre composites.

Using flax fibres as a reinforcement creates a complex material with several mechanical systems and interfacial regions. The main constituents are elementary flax fibres, having a hierarchic structure (SI Figure.I.a) leading to a complex mechanical behaviour [3] and bundles (SI Figure.I.c), aggregating several tens of elementary fibres, and coming from the original arrangement of fibres within a stem. These two main fibrous elements are also present in the composite structure and the associated interfaces regions needs to be taken into account [4]. An elementary flax fibre/polymer matrix interface is considered as the primary region of stress transfer between the matrix and the fibre [5]. A fibre/fibre

47 interphase is present in bundles; this is a 50 – 100 nm thick layer of peptic polymers [6]
48 linking fibres together, called the middle lamella. The importance of the middle lamella
49 should not be disregarded as it may be a zone of weakness in a composite material [7].
50 All these elements lead to a complex hierarchic composite structure, showed in SI
51 Figure.I.

52 Polyolefin polymers such as poly-(propylene) (PP) are commonly used with flax fibre
53 reinforcements [2], though these traditional thermoplastics, due to their petro-chemical
54 origin and limited end-of-life route (as recycling), have a limited ecological profile. With
55 the emergence of some bio-sourced and biodegradable polymers, it is relevant to examine
56 their potential as alternatives to traditional thermoplastics. Poly-(lactide) (PLA), poly-
57 (butylene-succinate) (PBS) and poly-(hydroxy alkanoate) (PHA) may replace PP due to
58 their excellent mechanical performance and their relative stability, even after a period of
59 garden composting [8]. Interestingly, all three of the biodegradable polymers (PLA, PHA,
60 PBS) have melting points under 200°C, allowing the manufacture of biocomposites
61 without damaging flax fibres [9]. Moreover, biodegradation can be an alternate end-of-life
62 scenario for these polymers as well as their flax reinforced biocomposites. However, it is
63 essential to look at the affinity between flax fibres and these polymers to understand the
64 feasibility of making effective biodegradable biocomposites, as well as appreciate their
65 mechanical properties.

66 This affinity is physically observed through the polymer/fibre interface, which can be
67 assessed from at least two scales [5]. At the micro-scale, one can measure the interfacial
68 shear strength (IFSS) of the interface between the fibre and polymer. Many protocols
69 exist, and have their own advantages and disadvantages [5]; the micro-droplet test [10] is
70 employed in this paper. One can also measure the performance of the interface at the

71 composite or macro-scale. A widely used test in composites science is the ±45° off-axis
72 tensile test developed and simplified by Rosen [11]. As it uses a unidirectional (UD) fibre
73 lay-up, it is more practical to conduct and is employed in this study.

74 For flax composites, it has been demonstrated at both scales, that epoxy resins have good
75 adherence to flax fibres [12]; recently, original matrices such as humins' resins [13] or
76 cellulose propionate [14] have also shown an interesting interfacial potential when used
77 with flax fibres . Regarding thermoplastic polymers, few research studies are available,
78 nevertheless, it is well-documented that PP presents a poor interface quality with flax, and
79 maleic-anhydride grafted PP (MAPP) is a standard solution to obtain a better interface
80 [15]. Due to its mechanical and ecological potential, interface of flax/PLA has been
81 explored and shown to be close to that of flax/epoxy resin [16]. To the authors'
82 knowledge, no articles have so far studied the interface between PHA or PBS and flax.

83 This study aims to characterise the interface at the micro-scale and determine its influence
84 on biocomposite properties, to assess whether heterogeneity of the mesostructure has any
85 role. Adhesion between fives thermoplastics (PP, MAPP, PLA, PHA, PBS) and flax fibre
86 is characterised by the micro-droplet method. $[\pm 45]_s$ in-plane shear tests and tensile tests
87 on unidirectional composites are also realised and compared with interfacial shear strength
88 to evaluate the role of the quality of the interface on biocomposite performance.

89 **2. Materials/methods:**

90 2.1. Materials

91 2.1.1. Materials

92 Light-weight unidirectional flax preforms (100 gsm), known as Flaxtape® and provided
93 by Ecotechnilin (Yvetot, France), were used to make composites. It is made of untwisted
94 flax fibres linked together by pectin [17]. To be consistent, elementary flax fibres used to

carry out micro-droplet tests were extracted from this preform. Three biodegradables polymers were used for this study: poly-(lactide) (PLA), poly-(butylene-succinate) (PBS) and poly-(hydroxy alkanoates) (PHA). Poly-(propylene) (PP) and maleic anhydride grafted poly-(propylene) (MAPP) were used as industry references. Supplier details and references are provided in SI Table I.

2.1.2. Composite manufacturing

As all the polymers investigated are thermoplastics, the film stacking process was used to manufacture the composite laminates. The methodology and parameters of both thermoplastic film processing and composite manufacturing were developed and detailed in a previous study [8] (SI Figure II). Flax preforms and polymer films were laid sequentially to make unidirectional and bi-axial composites, the orientation of flax fibres depending on the composite: $[0]_{16}$ for UD and $[\pm 45]_{8s}$ for bi-axial. A volume fraction of 32 ± 1% was achieved, calculated by a density method, i.e. through the exact weight and dimensions for each sample; then, fibre content was calculated by inverse method, knowing the fibre and matrix density. Results have been backed up by image analysis. Once these laminates were manufactured, they were cut with a milling machine. Samples with a shape based on ISO 527-4 for the $[\pm 45]_{8s}$ and ISO 527-5 for the $[0]_{16}$ were fabricated. Longitudinal 0° and transverse 90° samples were produced from the unidirectional laminates.

2.1.3. Micro-droplet sample manufacturing

Elementary flax fibres were extracted manually from the Flaxtape®. Some polymers wires were obtained by melting and rapidly stretching polymer films. A polymer wire was then manually fixed to an elementary fibre by making a double knot around the fibre (SI Figure III.a)). Finally, the system was put in an oven for 8 min at 200°C to melt the polymer

119 double knots and transform them into micro-droplets (SI Figure III.b)). The geometry of
120 every droplet was measured with an optical microscope. For each droplet, the length,
121 diameter and fibre diameter were obtained through an average of two measures. The
122 aspect ratio was extracted from these measures by dividing the length of the droplet by its
123 radius. The pictures used for the aspect ratio characterisation were analysed using a
124 software provided by *GBX* to identify the contact angle by a Song's method [18]. For each
125 formulation, contact angle and aspect ratio are mean value from at least 20 valid
126 measurements.

127 2.2. Methods

128 2.2.1. Micro-droplet tests

129 The elementary fibre/micro-droplet system was placed in a tensile machine equipped with
130 a 2 N load cell. The fibre is placed between two razor blades with the droplet just below
131 them. The fibre is pulled at a displacement rate of 0.1 mm/min, starting with the blades
132 locking the droplet, and continuing until debonding occurs (SI Figure III.c)). Load-
133 displacement curves were obtained (Figure 1.a). For each polymer, at least 20 samples
134 were tested to calculate the mean interfacial shear strength (IFSS). IFSS is commonly
135 obtained using equation (1), where F is the debonding force, L_d the length of the droplet
136 and D_f the diameter of the fibre.

$$\text{Interfacial shear strength} = \text{IFSS} = \frac{F_{debonding}}{A_{interface}} = \frac{F}{\pi . L_d D_f} \quad (1)$$

137 As recommended by Miller [10], the mean IFSS value in our study is obtained from a
138 linear regression analysis between the debonding load and the interface area (Figure 1b).

139 2.2.2. In-plane shear tests

140 The $[\pm 45]_{8s}$ samples were tensile tested at a displacement rate of 2 mm/min, on an Instron
141 machine equipped with a 10 kN load cell. An MTS biaxial extensometer was used to

record longitudinal and transverse strain. According to ASTM D 3518, the shear stress (τ_{12}) is given by (2) and the shear strain (γ_{12}) by (3), where *F* is the force applied, *S* is the sample section, ε_x and ε_y are the axial and transversal strain, respectively.

$$\tau_{12} = \frac{F}{2.S} = \frac{\sigma}{2} \quad (2)$$

$$\gamma_{12} = \varepsilon_x - \varepsilon_y \quad (3)$$

The shear behaviour was obtained by plotting shear stress versus shear strain. The in-plane shear strength (IPSS) was taken to be equal to the shear stress at a shear strain of 5%, as suggested by the standard. The shear modulus was recorded as supplementary data and calculated between a shear strain of 0.1% and 0.5%. For each formulation investigated, at least five samples were tested.

2.2.3. Tensile tests

Longitudinal 0° samples and transversal 90° samples were placed in an Instron machine, and tested at a cross-head speed of 1mm/min, using a 10 kN load cell. Tensile tests were carried out following ISO 527, and an Instron extensometer recorded strain in the loading direction. Strength and strain at failure were calculated. A tangent modulus for both orientations was calculated between a strain of 0.02 % and 0.1%. Furthermore, a second tangent modulus was recorded for the longitudinal samples at a strain of 0.6% to 0.8%. This threshold is taken when the modulus is stable whatever the formulation considered on this strain range. Indeed, it is known that UD flax composites have a bi-linear behaviour [19], in part due to the non-linear response of flax fibres, induce by its inner-structure [20]. For each formulation investigated, at least five samples were tested.

2.2.4. Scanning electronic microscopy

A JEOL SEM (JSM-IT500HRSEM) was used to observe the micro-droplet samples after debonding at an acceleration voltage of 3 kV. Transverse sections of UD composites were also observed. Gold sputter coating was carried out using a sputter coater (Scancoat6) from Edward.

3. Results:

3.1. Interfacial shear strength at micro-scale

Like other micro-scale interface tests, the micro-droplet test depends on several factors. The first step is to ensure that the studied systems are similar and therefore can be compared. For example, comparing results from studies with different operators, set-ups and sample manufacturing processes may be invalid, as these may have a significant influence on the droplet morphology and test result. These parameters stay constant in our systematic study of five different flax/polymer systems. Furthermore, the shape of the droplets has been scrutinised using microscopy to ensure mechanical results can be compared across the different flax/polymer systems. The contact angle of the droplet on the flax fibre and the droplet aspect ratio are presented in Table 1 and an example (on flax-PHA system) of typical debonding load-displacement curve, interfacial shear strength determination by linear regression and SEM images of droplet after debonding, is given in Figure 1. As both these parameters are comparable for all polymers, it is concluded that the shape of droplets may be regarded as similar.

Table 1

Furthermore, the rupture mechanism of the interfaces was observed by SEM. It was ascribed as interfacial shear failure (Mode II) for all polymers investigated here- see in Figure. 1.c and 1.d the case of PHA. This further ensures that the mechanical

polymer/fibre systems investigated can be compared. It is observed that PLA has an interface comparable to a poorly-adhered epoxy, as epoxy has a mean IFSS with flax of 18.6 ± 4.8 (mean value based on [12,16,21,22]) against 15.6 ± 2.7 for PLA/flax (based on our study). PHA, PBS and MAPP present similar IFSS with flax, though lower than that of PLA (Table 1). The effectiveness of maleic anhydride is exemplified by the fact that the IFSS of MAPP/flax is double that for PP/flax. Therefore, indeed, all bio-polymers have better or comparable adhesion with flax than MAPP and PP. This is explained by a higher surface tension for PLA/PHA/PBS than for PP/MAPP , see SI Table II, which leads a better power of adhesion. Furthermore, the surface of flax fibres presents many hydroxyl terminations. The presence of ester groups in these biopolymers allow some hydrogen bonds with flax surface, not found with PP. These hydrogen bonds are also present with MAPP due to the maleic-anhydride, explaining more comparable results.

Figure 1

3.2. In-plane shear strength at macro-scale

As fibre volume fraction influences the results from in-plane ± 45° shear test, we have ensured that samples have the same fibre content (Table 1). In-plane shear strength (IPSS) results follow the same trend as the interface at the microscale level; values are given in Table 1. PLA presents the best results, followed by PHA and then MAPP. PBS is slightly below MAPP but still higher than the industry reference, PP. Once again, the effectiveness of grafting PP with maleic anhydride to improve the interface with flax is observed. Note that the shear stress of PLA reaches a maximum value of 34.2 ± 1.0 MPa before shear strain is at 5%, leading to an IPSS of 33.2 ± 1.1 MPa.

The in-plane ± 45° shear test is an efficient and straightforward method to obtain IPSS. However, it is important to be aware that this test does not apply pure shear stress [23];

some inter-laminar stresses and inhomogeneous stress and strain distributions are present. Nevertheless, this test leads to a good approximation [23], which can be used to affirm that flax and biopolymer interfaces are better or comparable to MAPP and PP at the macro-scale, just like it was observed at the micro-scale.

3.3. Unidirectional composite characterisation

3.3.1. Transverse tensile behaviour

Unidirectional (UD) composites were characterised through transverse 90° tensile tests, to obtain the transverse modulus, strength and ultimate elongation. Focussing on the strength, it appears that flax/PLA presents the best transverse strength of 25.8 ± 1.0 MPa followed by PHA, PBS and MAPP (Table 1). As PP presents a lower strength than MAPP, the interface should have a role in the transverse tensile strength of the composite. This will be discussed in section 4.2.1, where the correlation between micro-scale and macro-scale interfacial and transverse strength is examined. Notice that samples submitted to a transverse tensile test present a significant concentration of strain in the matrix and at the interfaces [24]. This creates zones of high internal strains, damaging the material by generating micro-cracks. The eventual failure of the composites is due to the coalescing of these micro-cracks into (a) macro-crack(s). The matrices respond to these high local strains differently. Indeed, behaviour of the transverse-loaded composites (Figure 2.a)) is similar to the response of the corresponding raw polymer (SI Figure IV). Furthermore, there is a clear relation between the ultimate strain of the matrices and the ultimate strain of the transverse-loaded UD composites (Figure 2.b)).

Figure 2

The structure of a UD flax composite is more complex in comparison to that of a synthetic fibre composite (see Figure 3). In the former, the matrix is reinforced by elementary

fibres, which are not cylindrical or regular, as well as by larger irregular bundles. It is also possible to find some residual bast tissue due to the natural origin of flax fibres. All these elements generate a different strain concentration and distribution. Due to the random dispersion of these fibre elements in the matrix, the high strain distribution in the matrix becomes complex and can be locally high.

Figure 3

3.3.2. Longitudinal tensile behaviour

It is observed that the tensile behaviour of flax UD composites investigated is bilinear (see Figure 4). This bilinear behaviour was also observed for flax/unsaturated polyester and flax/epoxy composites [9,25]. Thus two stiffnesses ($E_{l,1}$ and $E_{l,2}$) were recorded, and for both, bio-polymers present at least comparable values to MAPP. All the results of the longitudinal tensile test are presented in Table 1. Regarding strength, PLA is followed by PHA and PBS, and all biopolymers possess composite strength higher than MAPP. Looking at the change of slope, it seems that the choice of the polymer does not influence the strain where the change in linearity takes place. As this phenomenon is not matrix dependent, it may be due to the behaviour of the fibre [9].

Figure 4

It is possible to back-calculate the fibre modulus using the rule-of-mixtures; results are presented in Table 1. Looking at results from the first composite stiffness ($E_{l,1}$), it appears that the back-calculated flax modulus obtained is close to literature value of 52.5 ± 8.6 GPa [26], for all considered polymer matrices.

4. Discussion

4.1. Influence of interface on composite shear strength

Two scales are of interest to obtain information on the interface(s). The micro-scale examines the adhesion between the polymer and elementary fibres through the IFSS, whereas the in-plane shear strength IPSS includes effects of the complex mesostructure of a flax composite, such as bundles, heterogeneity in fibre properties, possible remaining cortical components and fibre/fibre interphases. Both experiments show significant differences such as the scales investigated, fibre volume fractions used, and stress distribution generated. Nevertheless, as shown in Figure 5, there is a linear correlation between IFSS and IPSS. This indicates that adhesion between flax elementary fibres and the polymer is likely to be a crucial factor affecting in-plane shear strength. The in-plane shear strength IPSS presents a higher value than interfacial shear strength IFSS as the former does not only load interfaces, and presumably obtains higher contribution from fibres. Furthermore, this relation depends on the level of individualisation (i.e. ratio of elementary fibres to fibre bundles) of the preform. It is expected that a preform containing more bundles will deviate from this trend as the micro-droplet test was carried out on elementary fibres, and a bundle's behaviour would be more complex, according to the retting degree and the composition of fibre junctions.

Figure 5

The micro-droplet test focusses directly on the fibre/matrix interface, and therefore avoids influence by other factors (present at macro-scale tests). However, the theory is based on a critical assumption of linear stress along the interface [10]. It was demonstrated numerically [5,27] that there is a stress concentration where the razor blades lock the droplet. This stress concentration depends on the shape of the blade [27] and the distance

between the blades and the fibre [5,27]. As said previously, the blade shape does not scatter the results in our study as it stays unchanged. Despite the difficulty to validate the assumption of linear stress, the obtained values can be compared to each other.

On the other hand, in-plane shear $[\pm 45]_s$ test gives the in-plane shear strength of a composite taking into account its mesostructure. However, the test does not create pure shear as the matrix is also loaded. The composite quality has an essential role in the reliability of the results. The heterogeneity of the materials, such as matrix concentration zones and interlaminar zones may induce unwanted stress concentration. Nevertheless, as all these artefacts are present in a composite, this test reveals the "in-use" interface shear strength, which is more relevant for composite application [23].

4.2. Influence of interface on UD composite strength

4.2.1. Transverse strength

Generally speaking, whatever the reinforcement considered, the interface plays an essential role in the behaviour of a UD composite loaded transversally [28]. As shown in Figure 6, there is a clear correlation between the transverse strength of a UD composite and the in-plane shear strength characterising the interface. Indeed, the transverse loading of a UD composite induces high strain concentration at the interfaces [24]. It leads to damage in the composite through the generation of micro-cracks at the interfaces which coalesce to form (a) macro-crack(s) and eventually fracture the material. The appearance of micro-cracks depends on the ability of the interface to resist applied strain. If a matrix presents a better interface with fibre, the micro-cracks appear at a higher strain level, and higher applied stresses are needed to create some micro-cracks locally, thereby postponing the failure of the composite and leading to a higher ultimate strength. As mentioned previously, this analysis was done considering a matrix reinforced by elementary fibres,

being naturals or synthetics. In a flax composite, bundles also experience this strain concentration. In bundles, fibres are linked together by middle lamellae. It appears that the stiffness of middle lamellae is close to the transverse stiffness of flax fibres [29]. This natural feature found in a stem creates a remarkable cohesion inside bundles when it is loaded transversely, avoiding its decohesion. During retting, fibre extraction and composite manufacturing, this middle lamella is impacted, damaging this cohesion. In a composite submitted to transverse tensile loading, bundles act as fibres with a more prominent geometry but also as zones of weakness due to the damaged middle lamellae [30]. There is diversity in fibre forms (elementary, bundles) and level of heterogeneity in the UD composite due to the (random) dispersion of these fibre forms (Figure 3). The orientation of the bundles emerging from the manufacturing process can reconfigure the distribution of these high strain zones, thereby modifying the composite behaviour (SI Figure V). Despite considering the complexity of a flax composite, it appears clearly that the transverse strength is interface dependant.

Figure 6

4.2.2. Longitudinal strength

Estimating the longitudinal strength of a composite can be challenging, and many models are available. A modified rule of mixture is chosen here, which considers the matrix to be softer than the flax fibres, and therefore assumes failure is fibre-dominated. An effective parameter (k_{eff}) is added to match the model and the experiment empirically (4). This factor includes all fibre-related phenomena influencing the UD strength such as quality of fibre-matrix interface, distribution in fibre length and distribution in fibre (mis)orientation [31].

$$\sigma_{UD,l} = k_{eff}.V_f.\sigma_{fibre,l} + (1 - V_f)\sigma_{fiber,l}.\frac{E_m}{E_{fibre,l}} \quad (4)$$

V_f is the volume fraction of fibre, $\sigma_{UD,l}$ and $\sigma_{fibre,l}$ are respectively the longitudinal strength of the UD and the fibres, E_m and $E_{fibre,l}$ are the longitudinal stiffness of respectively the matrix and the fibre. Longitudinal strength and stiffness of flax fibre are taken respectively equal to 1,043 MPa and to 53.2 GPa as obtained by Bourmaud et al. with fibres extracted from the same preform [32].

It appears that the factor k_{eff} is interface dependant (Figure 7.a)), but is also influenced by the ultimate strain of the matrix (Figure 7.b)). Indeed, even though the interface between PBS and flax is of moderate quality (in comparison to the other polymers), the effective parameter of PBS is high; the moderate interface properties being balanced with the high ultimate strain of the PBS matrix. The reverse is true for PLA, where the effective parameter is principally due to the high quality of the interface (at low ultimate strain of PLA). Several hypotheses are proposed. If a matrix possesses a high ultimate strain, it may be able to spread the applied stress in the composite and avoid high-stress regions responsible for failure. Another explanation is that matrix is more resilient in high strain regions, such as at the ends of a fibre. It avoids the creation of micro-damage inside the material, yielding an increase in apparent strength. Indeed, even if the failure in flax UD composites is due to fibre failure, Monti et al. [33] observed matrix cracking before specimen rupture. In both assumptions, the explanation is related to the local stress and strain concentration inside the composite.

Figure 7

Some studies focus on developing the factor k_{eff} to express it clearly [34]. These models are not useable on UD flax composites as it is more complex than conventional composite

(Figure 8). In addition to the heterogeneous fibre distribution and the discontinuity of flax fibres (Figure 8.a)), the level of flax fibre individualisation also influences the strength of the composite [21]. More individualised fibres lead to higher strength, where bundles act as weaknesses inside the composite. This could be due to their lower aspect ratio or the higher stresses generated inside bundles. However, the second hypothesis is debatable due to the arrangement of fibres. As shown in Figure 8.c), flax fibres are discontinuous, but thanks to their intrusive growth in the stem, their diameter tapers and decreases at the ends [29]. These individual fibre ends increase the effectiveness of stress transfer between fibres through the middle lamellae. Besides, Coroller et al. [21] observed that individualisation leads to a larger increase in strength of a flax UD composite than obtained by selecting and using higher-strength fibres. As hackling is commonly used to extract flax fibres from stems, and it creates defects (*vis.* kink-bands) on fibres, a compromise has to be found between highly individualised fibres and undamaged fibres with higher strength.

Focussing on elementary flax fibres, they present a non-cylindrical section with an apparent diameter evolving along the fibre length [35] (Figure 8.b)). In addition to the geometric variability of flax fibres, it appears that fibre strength is dependent on the location in the stem they have been extracted from: fibres of highest strength are extracted from the middle of the stem [29]. A flax preform is typically made with a mix of these flax fibres, leading to dispersion in geometric, structural, and mechanical properties. Examining the same Flaxtape® used in our study, Gager et al. [36] observed a slight fibre misorientation. Fibres are oriented at approximatively 0° ± 15° with only 5% of fibre at 0°. In comparison, a commercial glass UD typically presented an orientation of 0° ± 10°

with 13% fibres at 0°. This higher misorientation for flax preforms penalises it against glass preforms, and impacts the strength of the final composite.

Figure 8

Despite the complexity of a UD flax composite, it appears that interfaces have an essential role in the stress transfer as well as the development of damage. The biodegradable polymers present higher interfacial properties with flax and lead to composites with higher mechanical properties than currently industrially used PP and even MAPP.

5. Conclusion

The interface between flax and three biodegradable polymers (PLA, PHA, PBS) was investigated at the micro-scale and compared to PP and MAPP, two industry references. It is demonstrated that the adhesion and interfacial shear strength of biodegradable polymers to flax is at least as good as MAPP, and more than twice that of PP. A mechanical investigation at the composite scale is realised through in-plane shear tests and tensile tests on unidirectional composites. The macro-scale in-plane shear strength, the longitudinal tensile strength and the transversal tensile strength follow the same trend for fibre/matrix adhesion observed at the micro-scale through micro-droplet tests: flax composites made from biopolymers are at least as good as MAPP/flax composites, with the best values for PLA/flax composites. A comparison is carried out between interfacial properties and composite mechanical properties. It appears that the in-plane shear strength of the composite and the UD transversal strength correlate linearly. In the longitudinal direction, the strength depends on fibre-matrix adhesion, but also on the ultimate strain at failure of the matrix. Based on this analysis and due to the good adherence between flax fibres and biodegradable polymers, it is evident that biopolymers should be exploited as alternatives to thermoplastic polyolefins as they present interesting mechanical properties and lead to

recyclable and compostable mid-performance materials. In the future, it is imperative to explore the correlation between fibre-matrix adhesion, mechanical behaviour (such as fatigue), composite architecture (such as fibre volume fraction), and durability (including biodegradation).

Acknowledgements

This work was funded by the Interreg V.A Cross-Channel Programme through the project FLOWER: Flax composites, LOW weight, End of life and Recycling (Grant Number 23).

References

[1] S.V. Joshi, L.T. Drzal, A.K. Mohanty, S. Arora, Are natural fiber composites environmentally superior to glass fiber reinforced composites?, Composites Part A: Applied Science and Manufacturing. 35 (2004) 371–376. https://doi.org/10.1016/j.compositesa.2003.09.016.

[2] A. Bourmaud, J. Beaugrand, D.U. Shah, V. Placet, C. Baley, Towards the design of high-performance plant fibre composites, Progress in Materials Science. 97 (2018) 347–408. https://doi.org/10.1016/j.pmatsci.2018.05.005.

[3] A. Lefeuvre, A. Bourmaud, C. Morvan, C. Baley, Elementary flax fibre tensile properties: Correlation between stress–strain behaviour and fibre composition, Industrial Crops and Products. 52 (2014) 762–769. https://doi.org/10.1016/j.indcrop.2013.11.043.

[4] C. Baley, A. Le Duigou, A. Bourmaud, P. Davies, Reinforcement of polymers by flax fibres: The role of interfaces. Chapitre de l'ouvrage: Bio-based Composites for High-Performance Materials: From Strategy to Industrial application. Editors: W. Smitthipong, R. Chollakup, M. Nardin, 2014, Taylor and Francis, 2014.

[5] P.J. Herrera-Franco, L.T. Drzal, Comparison of methods for the measurement of fibre/matrix adhesion in composites, Composites. 23 (1992) 2–27. https://doi.org/10.1016/0010-4361(92)90282-Y.

[6] M.S. Zamil, A. Geitmann, The middle lamella—more than a glue, Phys. Biol. 14 (2017) 015004. https://doi.org/10.1088/1478-3975/aa5ba5.

[7] K. Charlet, A. Béakou, Mechanical properties of interfaces within a flax bundle – Part I: Experimental analysis, International Journal of Adhesion and Adhesives. 31 (2011) 875–881. https://doi.org/10.1016/j.ijadhadh.2011.08.008.

[8] D. Pantaloni, D. Shah, C. Baley, A. Bourmaud, Monitoring of mechanical performances of flax non-woven biocomposites during a home compost degradation, Polymer Degradation and Stability. (2020) 109166. https://doi.org/10.1016/j.polymdegradstab.2020.109166.

[9] C. Baley, A. Le Duigou, A. Bourmaud, P. Davies, Influence of drying on the mechanical behaviour of flax fibres and their unidirectional composites, Composites Part A: Applied Science and Manufacturing. 43 (2012) 1226–1233. https://doi.org/10.1016/j.compositesa.2012.03.005.

[10] B. Miller, P. Muri, L. Rebenfeld, A microbond method for determination of the shear strength of a fiber/resin interface, Composites Science and Technology. 28 (1987) 17–32. https://doi.org/10.1016/0266-3538(87)90059-5.

[11] B.W. Rosen, A simple procedure for experimental determination of the longitudinal shear modulus of unidirectional composites, Journal of Composite Materials. 6 (1972) 552–554.

[12] A. Le Duigou, P. Davies, C. Baley, Exploring durability of interfaces in flax fibre/epoxy micro-composites, Composites Part A: Applied Science and Manufacturing. 48 (2013) 121–128. https://doi.org/10.1016/j.compositesa.2013.01.010.

[13] A. Sangregorio, N. Guigo, J.C. van der Waal, N. Sbirrazzuoli, All ‘green’ composites comprising flax fibres and humins’ resins, Composites Science and Technology. 171 (2019) 70–77. https://doi.org/10.1016/j.compscitech.2018.12.008.

[14] W. Woigk, C.A. Fuentes, J. Rion, D. Hegemann, A.W. van Vuure, E. Kramer, C. Dransfeld, K. Masania, Fabrication of flax fibre-reinforced cellulose propionate

thermoplastic composites, Composites Science and Technology. 183 (2019) 107791. https://doi.org/10.1016/j.compscitech.2019.107791.

[15] M.H. Akonda, H.M. El-Dessouky, Effect of Maleic-Anhydride Grafting on the Properties of Flax Reinforced Polypropylene Textile Composites, Journal of Textile Science and Technology. 05 (2019) 69. https://doi.org/10.4236/jtst.2019.54007.

[16] A. Le Duigou, P. Davies, C. Baley, Interfacial bonding of Flax fibre/Poly(l-lactide) bio-composites, Composites Science and Technology. 70 (2010) 231–239. https://doi.org/10.1016/j.compscitech.2009.10.009.

[17] M. Khalfallah, B. Abbès, F. Abbès, Y.Q. Guo, V. Marcel, A. Duval, F. Vanfleteren, F. Rousseau, Innovative flax tapes reinforced Acrodur biocomposites: A new alternative for automotive applications, Materials & Design. 64 (2014) 116–126. https://doi.org/10.1016/j.matdes.2014.07.029.

[18] B. Song, A. Bismarck, R. Tahhan, J. Springer, A Generalized Drop Length–Height Method for Determination of Contact Angle in Drop-on-Fiber Systems, Journal of Colloid and Interface Science. 197 (1998) 68–77. https://doi.org/10.1006/jcis.1997.5218.

[19] D.U. Shah, Damage in biocomposites: Stiffness evolution of aligned plant fibre composites during monotonic and cyclic fatigue loading, Composites Part A: Applied Science and Manufacturing. 83 (2016) 160–168. https://doi.org/10.1016/j.compositesa.2015.09.008.

[20] I. Burgert, P. Fratzl, Plants control the properties and actuation of their organs through the orientation of cellulose fibrils in their cell walls, Integr Comp Biol. 49 (2009) 69–79. https://doi.org/10.1093/icb/icp026.

[21] G. Coroller, A. Lefeuvre, A. Le Duigou, A. Bourmaud, G. Ausias, T. Gaudry, C. Baley, Effect of flax fibres individualisation on tensile failure of flax/epoxy unidirectional composite, Composites Part A: Applied Science and Manufacturing. 51 (2013) 62–70. https://doi.org/10.1016/j.compositesa.2013.03.018.

475 [22] L. Marrot, A. Bourmaud, P. Bono, C. Baley, Multi-scale study of the adhesion
476 between flax fibers and biobased thermoset matrices, Materials & Design (1980-
477 2015). 62 (2014) 47–56. https://doi.org/10.1016/j.matdes.2014.04.087.
478 [23] C.C. Chiao, R.L. Moore, T.T. Chiao, Measurement of shear properties of fibre
479 composites: Part 1. Evaluation of test methods, Composites. 8 (1977) 161–169.
480 https://doi.org/10.1016/0010-4361(77)90011-8.
481 [24] I.M. Daniel, O. Ishai, Engineering mechanics of composite materials, 2nd ed, Oxford
482 University Press, New York, 2006.
483 [25] D.U. Shah, P.J. Schubel, M.J. Clifford, P. Licence, The tensile behavior of off-axis
484 loaded plant fiber composites: An insight on the nonlinear stress-strain response,
485 Polymer Composites. 33 (2012) 1494–1504. https://doi.org/10.1002/pc.22279.
486 [26] C. Baley, A. Bourmaud, Average tensile properties of French elementary flax fibers,
487 Materials Letters. 122 (2014) 159–161. https://doi.org/10.1016/j.matlet.2014.02.030.
488 [27] G. Pandey, C.H. Kareliya, R.P. Singh, A study of the effect of experimental test
489 parameters on data scatter in microbond testing, Journal of Composite Materials. 46
490 (2012) 275–284. https://doi.org/10.1177/0021998311410508.
491 [28] K. Benzarti, L. Cangemi, F. Dal Maso, Transverse properties of unidirectional
492 glass/epoxy composites: influence of fibre surface treatments, Composites Part A:
493 Applied Science and Manufacturing. 32 (2001) 197–206.
494 https://doi.org/10.1016/S1359-835X(00)00136-6.
495 [29] C. Baley, C. Goudenhooft, M. Gibaud, A. Bourmaud, Flax stems: from a specific
496 architecture to an instructive model for bioinspired composite structures, Bioinspir.
497 Biomim. 13 (2018) 026007. https://doi.org/10.1088/1748-3190/aaa6b7.
498 [30] V. Mazzanti, R. Pariante, A. Bonanno, O. Ruiz de Ballesteros, F. Mollica, G.
499 Filippone, Reinforcing mechanisms of natural fibers in green composites: Role of
500 fibers morphology in a PLA/hemp model system, Composites Science and
501 Technology. 180 (2019) 51–59. https://doi.org/10.1016/j.compscitech.2019.05.015.

[31] J. Gironès, J.P. Lopez, F. Vilaseca, J. Bayer R., P.J. Herrera-Franco, P. Mutjé, Biocomposites from Musa textilis and polypropylene: Evaluation of flexural properties and impact strength, Composites Science and Technology. 71 (2011) 122–128. https://doi.org/10.1016/j.compscitech.2010.10.012.

[32] A. Bourmaud, A. Le Duigou, C. Gourier, C. Baley, Influence of processing temperature on mechanical performance of unidirectional polyamide 11–flax fibre composites, Industrial Crops and Products. 84 (2016) 151–165. https://doi.org/10.1016/j.indcrop.2016.02.007.

[33] A. Monti, A. El Mahi, Z. Jendli, L. Guillaumat, Mechanical behaviour and damage mechanisms analysis of a flax-fibre reinforced composite by acoustic emission, Composites Part A: Applied Science and Manufacturing. 90 (2016) 100–110. https://doi.org/10.1016/j.compositesa.2016.07.002.

[34] M.R. Piggott, M. Ko, H.Y. Chuang, Aligned short-fibre reinforced thermosets: Experiments and analysis lend little support for established theory, Composites Science and Technology. 48 (1993) 291–299. https://doi.org/10.1016/0266-3538(93)90146-8.

[35] K. Charlet, C. Baley, C. Morvan, J.P. Jernot, M. Gomina, J. Bréard, Characteristics of Hermès flax fibres as a function of their location in the stem and properties of the derived unidirectional composites, Composites Part A: Applied Science and Manufacturing. 38 (2007) 1912–1921. https://doi.org/10.1016/j.compositesa.2007.03.006.

[36] V. Gager, D. Legland, A. Bourmaud, A. Le Duigou, F. Pierre, K. Behlouli, C. Baley, Oriented granulometry to quantify fibre orientation distributions in synthetic and plant fibre composite preforms, Industrial Crops and Products. 152 (2020). https://doi.org/10.1016/j.indcrop.2020.112548.

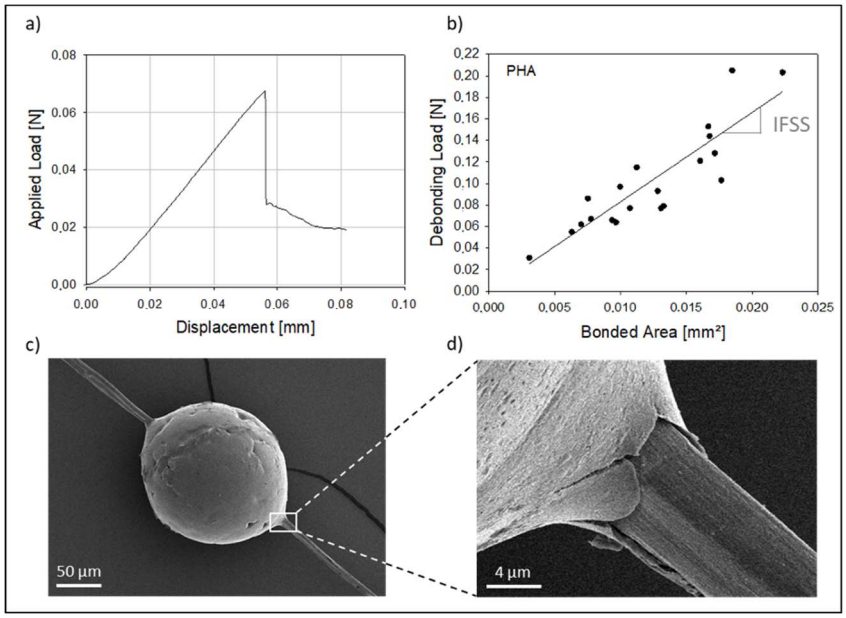

Figure 1: a) Typical response of a flax/PHA droplet system undergoing a micro-droplet test; b) Mean interfacial shear strength determination by linear regression of PHA bonded to elementary flax fibre; c)-d) PHA droplet on an elementary flax fibre with a zoomed image showing the interface failing through mode II.

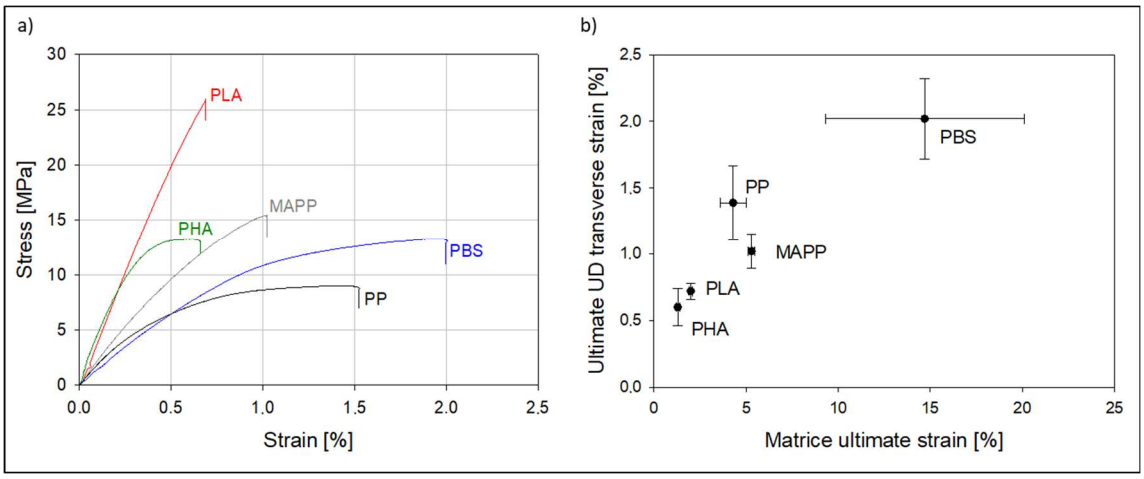

Figure 2: a) Transverse tensile behaviour of UD flax composites at a volume fraction of 32%, b) relation between the ultimate transverse strain of flax composites and the ultimate strain of the corresponding matrices.

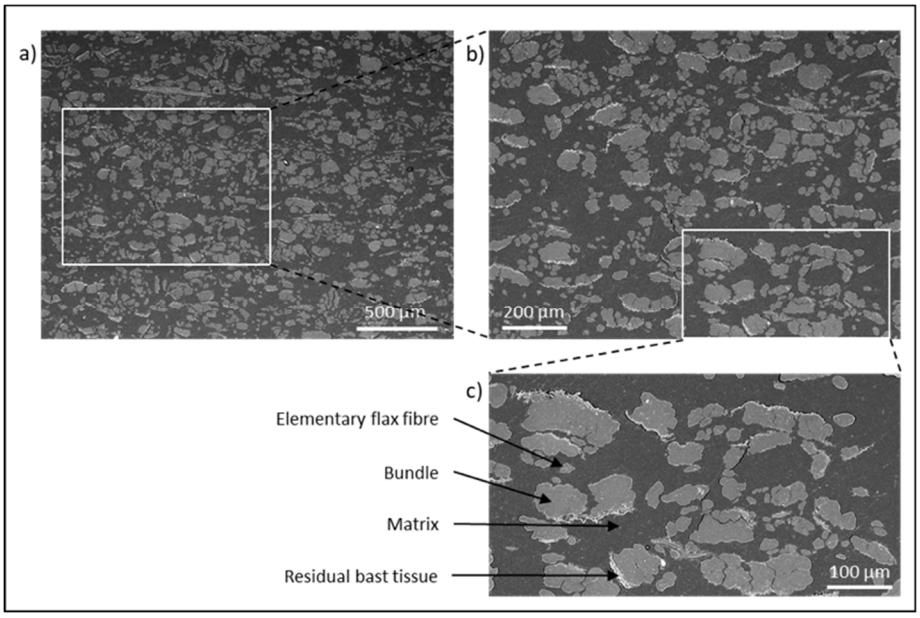

536

537 Figure 3: Sliced observation of an MAPP/flax composite at several scales.

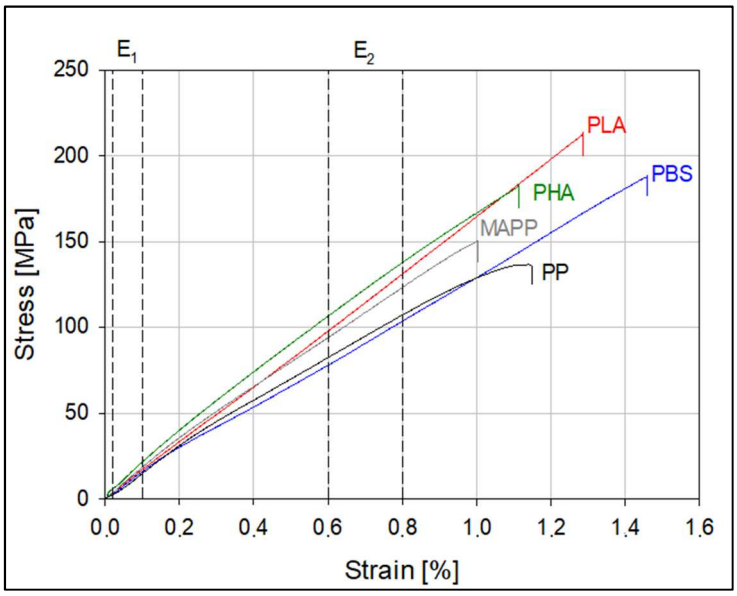

538

539 Figure 4: Longitudinal tensile behaviour of unidirectional flax composites. The dotted

540 line indicates the strain range for modulus calculation.

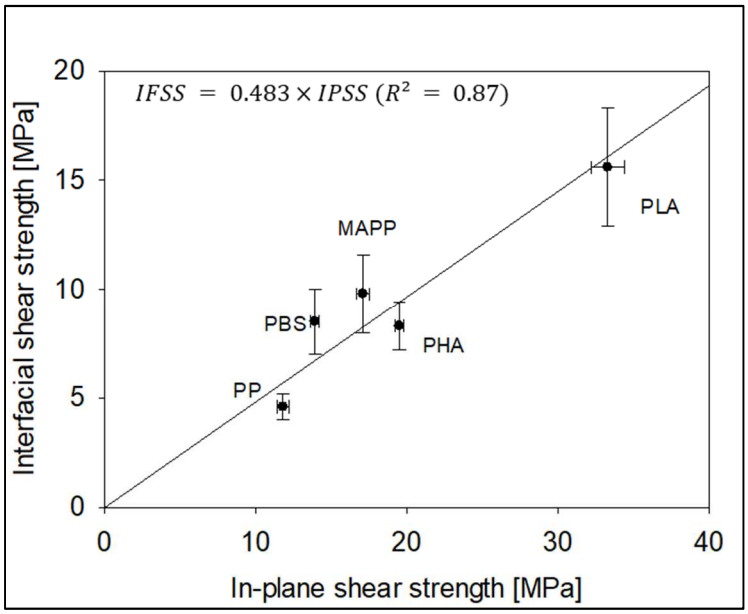

541

542 Figure 5: Linear correlation between the interfacial shear strength IFSS measured at the
543 micro-scale and the in-plane shear strength IPSS measured at macro-scale for
544 flax/thermoplastic composite systems.

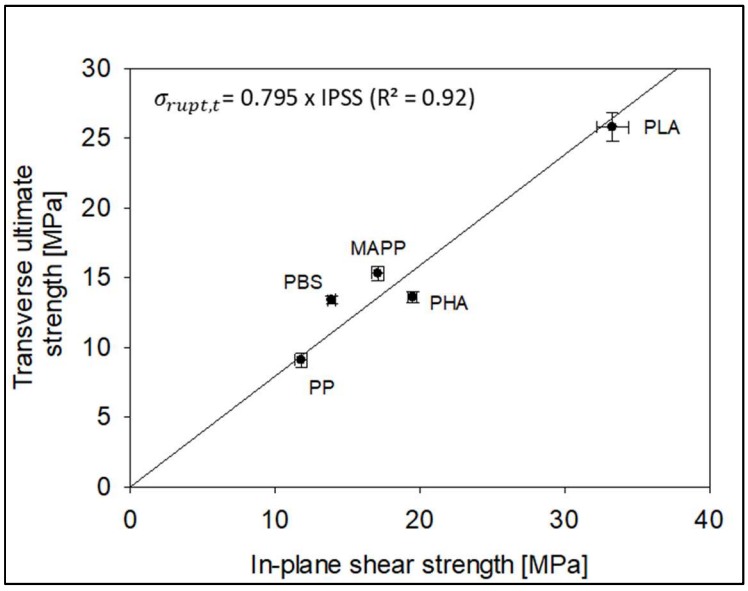

545

546 Figure 6: Correlation between the in-plane shear strength IPSS and the ultimate transverse
547 strength of unidirectional flax composites.

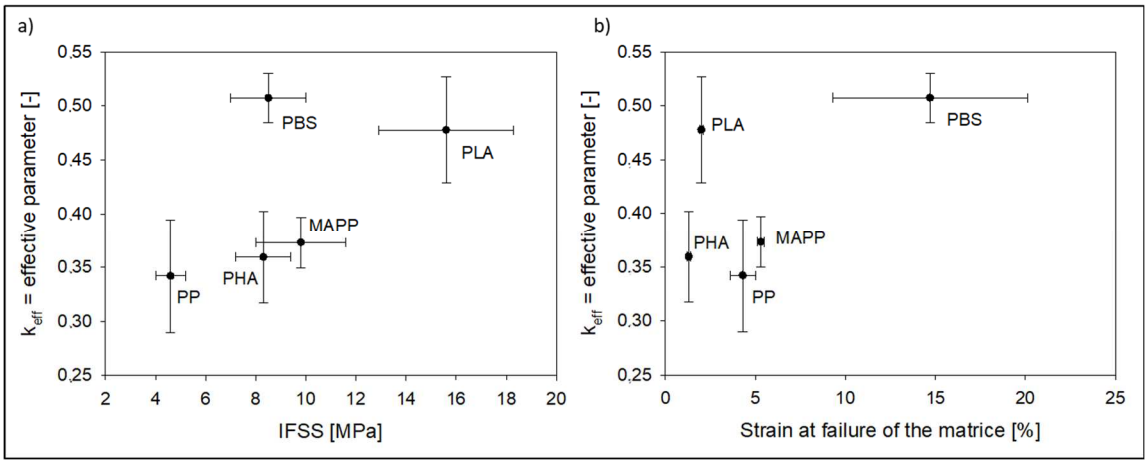

548

549 Figure 7: Effective parameter (k_{eff}) of the fibre contribution at longitudinal strength in

550 function of a) the interfacial shear strength, b) strain at failure of matrices.

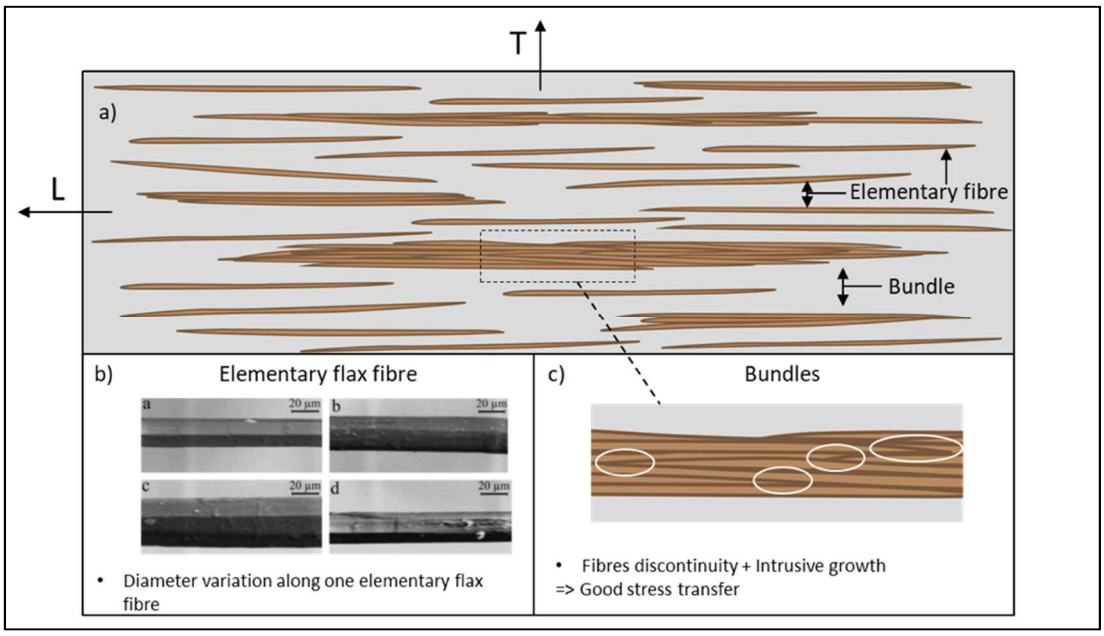

551

552 Figure 8: a) Schema of a top inner view of a flax UD composite portraying the

553 misorientation, the presence of bundles as well as discontinuous elementary fibres. L and

554 T represent the longitudinal and transversal directions. For the purposes of clarity, the

555 aspect ratio of the fibre is not to scale. b) SEM images extracted from [35] showing the

556 diameter evolution of elementary flax fibre, c) Schema of a bundle focussing on the fibre

557 discontinuities inside the bundles.

558 Table 1: Mechanical characterisation of flax composites at various scales: micro-droplet

559 test, in-plane shear test, and tensile test on unidirectional composite in both directions.

560 * $E_{l,1}$ is calculated from a strain of 0.02% to 0.1% and $E_{l,2}$ from 0.6% to 0.8%.

		PLA	PHA	PBS	MAPP	PP
Micro-droplet test	Contact angle [°]	69.3 ± 3.5	66.1 ± 7.5	72.3 ± 4.1	64.3 ± 4.6	67.7 ± 5.2
	$L_{droplet}/D_{droplet}$ [-]	1.28 ± 0.08	1.32 ± 0.09	1.24 ± 0.07	1.33 ± 0.14	1.33 ± 0.09
	IFSS [MPa]	15.6 ± 2.7	8.3 ± 1.1	8.5 ± 1.5	9.8 ± 1.8	4.6 ± 0.6
In-plane shear test on $[\pm 45]_s$	V_f [%]	32.2 ± 0.4	30.2 ± 0.9	30.4 ± 0.8	30.6 ± 0.4	32.3 ± 0.4
	G_{lt} [MPa]	1756 ± 64	1286 ± 16	572 ± 25	806 ± 18	654 ± 24
	IPSS [MPa]	33.2 ± 1.1	19.4 ± 0.3	13.9 ± 0.3	17.1 ± 0.3	12.0 ± 0.0(4)
	τ_{max}[MPa]	34.2 ± 1.0	-	-	-	-
	γ_{max} [%]	3.1 ± 0.2	-	-	-	-
Tensile test on matrices (from [3])	E_m [GPa]	3.8 ± 0.1	4.4 ± 0.3	0.75 ± 0.1	1.58 ± 0.05	1.4 ± 0.2
	$\sigma_{rupt,m}$ [MPa]	61.4 ± 0.8	38.6 ± 1.4	39.1 ± 0.5	25.1 ± 0.1	24.4 ± 0.8
	$\varepsilon_{rupt,m}$ [%]	2.0 ± 0.1	1.3 ± 0.1	14.7 ± 5.4	5.3 ± 0.2	4.3 ± 0.7
UD parameter	V_f [%]	33.5 ± 0.2	33.2 ± 0.5	32.9 ± 0.25	33.0 ± 0.8	31.7 ± 0.7
Transversal tensile test on UD	E_t [GPa]	4.2 ± 0.4	3.9 ± 0.9	1.5 ± 0.1	2.5 ± 0.3	2.0 ± 0.2
	$\sigma_{rupt,t}$ [MPa]	25.8 ± 1.0	13.6 ± 0.4	13.4 ± 0.3	15.3 ± 0.5	9.1 ± 0.5
	$\varepsilon_{rupt,t}$ [%]	0.72 ± 0.06	0.60 ± 0.14	2.02 ± 0.30	1.02 ± 0.13	1.39 ± 0.28
Longitudinal tensile test on UD	$E_{l,1}$ [GPa] *	20.1 ± 2.8	20.3 ± 3.1	16.9 ± 2.5	17.8 ± 2.8	17.9 ± 4.3
	$E_{l,2}$ [GPa] *	16.3 ± 0.9	14.8 ± 1.1	13.7 ± 1.3	13.4 ± 2.1	11.9 ± 1.6
	$\sigma_{rupt,l}$ [MPa]	216 ± 17	182 ± 13	184 ± 9	151 ± 9	133 ± 17
	$\varepsilon_{rupt,l}$ [%]	1.30 ± 0.16	1.13 ± 0.10	1.36 ± 0.15	0.99 ± 0.07	1.14 ± 0.19
Back calculation using a ROM	E_{fibre} [GPa] using $E_{l,1}$	59.8 ± 8.3	60.9 ± 9.3	51.6 ± 7.7	53.8 ± 7.4	55.9 ± 13.7
	E_{fibre} [GPa] using $E_{l,2}$	48.5 ± 2.4	44.4 ± 3.0	41.6 ± 4.0	40.4 ± 5.8	29.5 ± 16.1

561

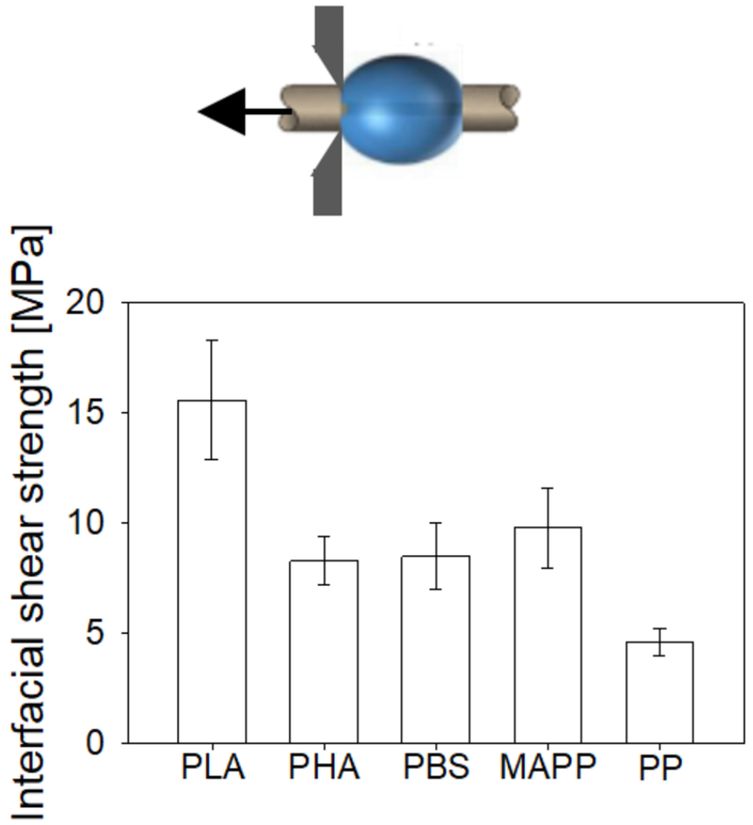
Interfacial shear strength [MPa]
20
15
10
5
0
PLA
PHA
PBS
MAPP
PP

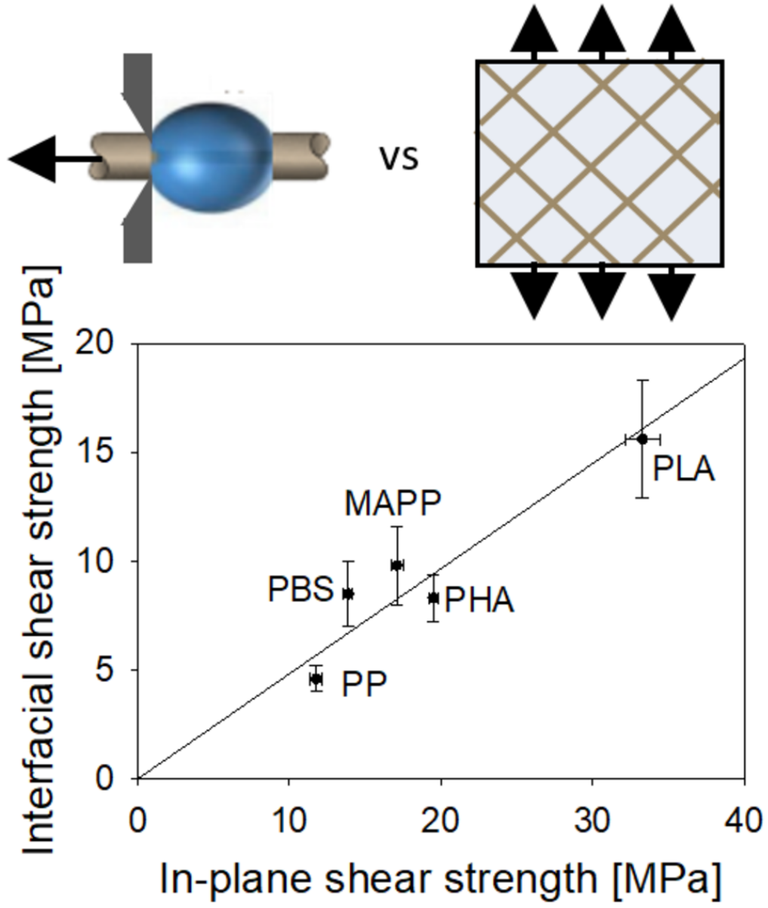
vs
Interfacial shear strength [MPa]
20
15
10
5
0
0
10
20
30
40
In-plane shear strength [MPa]
PLA
MAPP
PBS
PHA
PP

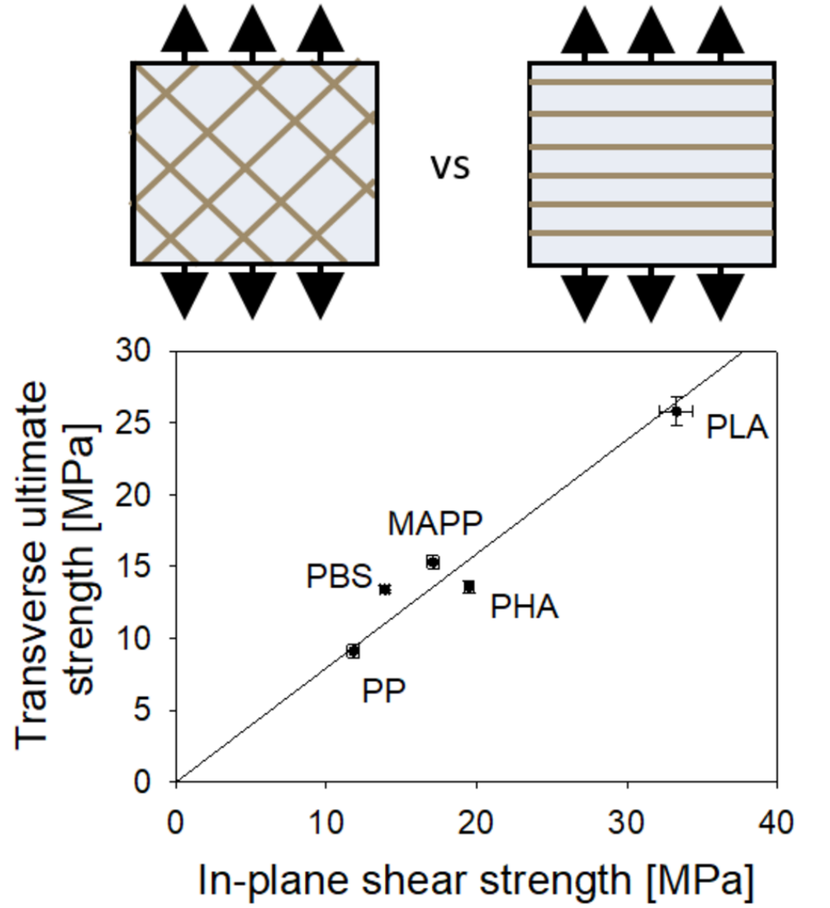
vs
Transverse ultimate strength [MPa]
30
25
20
15
10
5
0
0
10
20
30
40
In-plane shear strength [MPa]
PLA
MAPP
PBS
PHA
PP